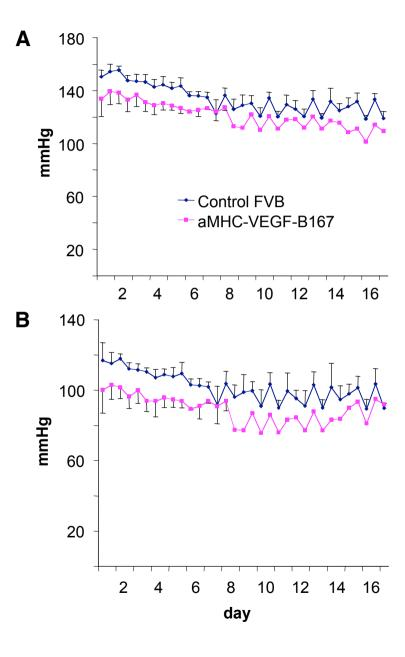
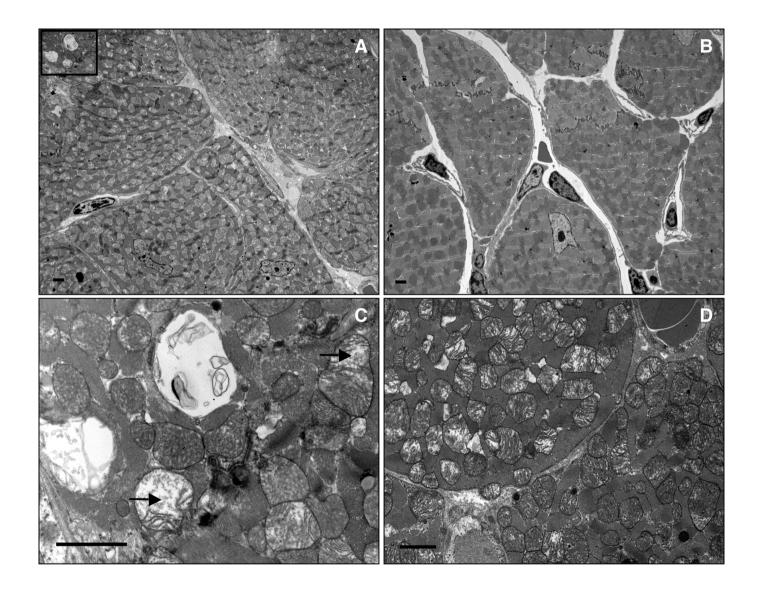
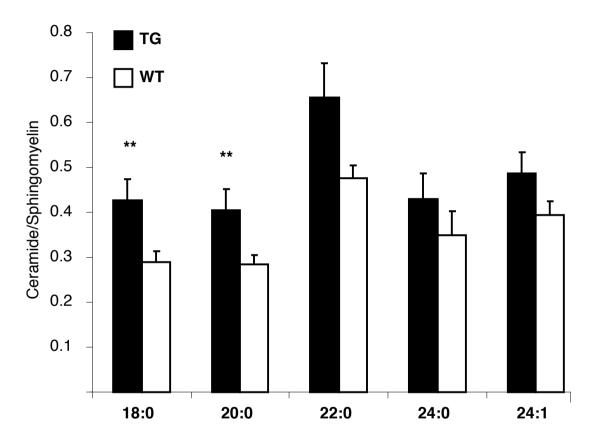


Karpanen et al., Supplemental Figure 1







## **Supplemental Figure Legends**

Supplemental Figure 1. Expression of the transgenes and minimal angiogenic effects of VEGF-B on skin vasculature. (A) The expression of the K14-VEGF-B transgene was analyzed by Northern blotting of RNA isolated from the skin of the K14-VEGF-B and littermate control mice with a probe recognizing VEGF-B mRNA. (B) The proper expression of the K14-VEGF-B transgene was confirmed by immunohistochemistry of paraffin sections of the skin with antibodies against mouse VEGF-B. The skin vasculature was analyzed by whole-mount staining of ear skin with antibodies against the panendothelial marker Pecam-1. (C) Number of Pecam-1 stained vessels and their branching points per microscopic high-power field (hpf). \*\*, p < 0.05. (D) The expression of the  $\alpha$ MyHC-VEGF-B<sub>167</sub> transgene was analyzed by RT-PCR (left) and Northern blotting (right) of RNA isolated from the hearts of  $\alpha$ MyHC-VEGF-B<sub>167</sub> and littermate control mice.

Supplemental Figure 2. Telemetric analysis of blood pressure. Day- and night-time systolic (**A**) and diastolic (**B**) blood pressure of  $\alpha$ MyHC-VEGF-B<sub>167</sub> and wild type mice as a function of time. Note the decreasing trend in the blood pressure after the probe insertion procedure (on day 0).

Supplemental Figure 3. Analysis of mitochondrial changes in the hearts of  $\alpha MyHC$ -VEGF- $B_{167}$  mice by electron microscopy. Transmission electron micrographs displaying mitochondrial morphology in the hearts of six-month-old  $\alpha MyHC$ -VEGF- $B_{167}$  (**A**) and wildtype (**B**) mice. (**C**) Magnification of boxed area in A, featuring accumulating vacuoles and swollen mitochondria with altered cristae (arrows). (**D**) Electron micrograph from a two-month-old  $\alpha MyHC$ -VEGF- $B_{167}$  mouse heart showing progressive mitochondrial degeneration. Scale bar = 2  $\mu m$ .

Supplemental Figure 4. Levels of cardiac ceramides with different acyl chain lengths. The ratio of ceramides to sphingomyelin in the hearts of female  $\alpha$ MyHC-VEGF-B<sub>167</sub> and wild type mice. \*\*, p < 0.05.

## **Supplemental Results**

*VEGF-B is minimally angiogenic in transgenic mouse skin.* Previous studies have shown that when overexpressed under the K14 promoter in transgenic mouse skin, VEGF and PIGF induce an angiogenic phenotype and VEGF-C and VEGF-D a lymphangiogenic phenotype<sup>1-4</sup>. We generated transgenic mice overexpressing VEGF-B under the K14 promoter and confirmed transgene expression by Northern blotting and immunohistochemistry (Supplemental Figure 1, A-B). The mice developed normally, appeared healthy, were fertile, and had a normal life span. The skin of the ears, snout and paws had a normal pinkish blush, and hair growth over the body was normal, without any signs of spontaneous skin lesions or abnormalities, for up to 1.5 years of age. VEGF-B overexpression only slightly increased vessel density ( $42 \pm 5$  vessels/mm<sup>2</sup> in K14-VEGF-B mice versus  $35 \pm 4$  vessels/mm<sup>2</sup> in WT mice, n = 10, p < 0.05) and vessel branching ( $392 \pm 74$  branchpoints/mm<sup>2</sup> in K14-VEGF-B mice versus  $331 \pm 54$  branchpoints/mm<sup>2</sup> in WT mice, n = 7, p < 0.05) in the skin (Supplemental Figure 1C). These vessels had a normal morphology, size, patterning and mural cell coating as analyzed by immunostaining for smooth muscle alpha-actin (SMA; data not shown). Thus, VEGF-B only minimally promoted angiogenesis when overexpressed in the skin.

## **Supplemental Materials and Methods**

Generation of the transgenic mice. To generate the K14-VEGF-B transgenic mice, DNA from the human VEGF-B gene corresponding to nucleotides 745-5059 of Genbank accession number AF468110 was cloned into the K14 expression vector (kindly provided by Dr. Elaine Fuchs<sup>5</sup>), and one non-initiating upstream ATG was mutated into a GTG. The expression cassette was excised from the vector backbone and injected into fertilized mouse oocytes of FVB background. The mice were PCR-genotyped using tail DNA with the primers 5'-TCTCCCAGCCTGATGCCCCT-3' and 5'-GGACTTGGTGCTGCCCAGTG-3'.

To generate a heart specific transgene, the recessed 3'-ends of the EcoRI fragment from a human VEGF-B<sub>167</sub>/pCRII vector<sup>6</sup> were filled in with the Klenow fragment of DNA polymerase I and ligated to the Sal I-opened and Klenow filled-in αMyHC promoter expression vector (a kind gift from Dr. Jeffrey Robbins). The expression cassette was excised from the vector backbone with BamHI and injected into fertilized mouse oocytes of FVB background. The mice were genotyped by PCR of tail DNA with the primer pair 5'-TCTCCCAGCCTGATGCCCCT-3' and 5'-GCCATGTGTCACCTTCGCAG-3'.

The expression of the transgene was confirmed by subjecting total RNA to Northern blotting and hybridization with a <sup>32</sup>P-labeled VEGF-B cDNA probe (nucleotides 1-382, Genbank Accession No U48800), by RT-PCR using the primer pair 5'-TCTCCCAGCCTGATGCCCCT-3' and 5'-CTAAGCCCCGCCCTTGGC-3', and by immunohistochemistry and Western blotting. The phenotypes were analyzed from two αMyHC-VEGF-B founder lines expressing the transgene. All experiments involving mice were approved by the Provincial State Office of Southern Finland and carried out in accordance with institutional guidelines.

Immunohistochemistry. For quantification of blood vessels in the heart, 7 μm sections of 4% paraformaldehyde (PFA) fixed, paraffin-embedded mouse tissues were deparaffinized, rehydrated, and pretreated with trypsin (0.25 mg/ml trypsin in 9 mM CaCl<sub>2</sub>, 50 mM Tris pH 7.8) for 30 minutes at 37°C, and the endogenous peroxidase was inactivated with 3% H<sub>2</sub>O<sub>2</sub> in methanol. After blocking, the slides were incubated with purified rat anti-mouse Pecam-1 (MEC13.3, BD Pharmingen) at a concentration of 0.625 μg/ml overnight at +4°C, washed, and incubated with biotinylated rabbit anti-rat IgG at a concentration of 1.7 μg/ml (BA-4001, Vector Laboratories) for 30 min at room temperature. The slides were stained using the TSA-kit (NEN Life Sciences/PerkinElmer Life and Analytical Sciences) according to the manufacturer's instructions. The number and size of the Pecam-1 stained vessels were quantified from four photomicrographs per mouse photographed with an Olympus AX70 microscope and DP50 Camera (Olympus) using the ImageJ program (National Institutes of Health). The number of Pecam-1 positive endothelial cell nuclei per blood vessel cross-section was quantified using Pecam-1/hematoxylin staining (four photomicrographs per mouse). Results are expressed as average ± SD.

8 μm cryosections of frozen tissues were fixed in acetone, blocked, and incubated with rabbit antimouse collagen IV (Cosmo Bio), rabbit anti-laminin-1 antiserum (a kind gift from Päivi Liesi), anti-rat VEGFR-1 (5B12, ImClone Systems Incorporated), goat anti-rat neuropilin-1 (AF566, R&D Systems) or goat anti-human VEGF-B (AF751, R&D Systems) primary antibodies for 2 hours. Intracellular VEGF-B staining was observed when using microwave pretreatment of slides in DakoCytomation Low pH Target Retrieval Solution. AlexaFluor488-conjugated anti-rabbit and AlexaFluor594-conjugated anti-goat (Molecular Probes) antibodies were used for detection. Zeiss Axioplan2 epifluorescence microscope (Zeiss) was used for imaging. Cardiomyocyte sizes in transgenic and control hearts were

quantified from four correspondingly located laminin-1 stained high-power field photomicrographs per heart using the Axiovision program (Zeiss).

Mouse ears were dissected for whole-mount immunostaining, fixed in 4% PFA, and incubated with antibodies against Pecam-1, followed by detection with peroxidase-labeled IgGs (Dako). For quantification of branch points and vessel densities, 24 optical fields (400x) per mouse, sampled randomly in the center and periphery of the ear, were photographed with a digital camera. For quantification of vessel densities, prints of the images were divided by horizontal lines into five equal sectors and all crossing points of the vessels with the horizontal lines were counted. Vessel branching was quantified from the same prints by counting the branch points. Values are presented as average ± SD.

Echocardiography. Transthoracic echocardiography was performed using an Acuson Ultrasound System (Sequoia<sup>TM</sup> 512) and a 15-MHz linear transducer (15L8) (Acuson) or a VEVO 779 Ultrasound System (VisualSonics). Mice were anesthetized with fentanyl citrate 8  $\mu$ g/10 g, fluanisone 250  $\mu$ g/10 g and midazolam 125  $\mu$ g/10 g. Normal body temperature was maintained during the examination with a warming pad and lamp.

Using two-dimensional imaging, a short axis view of the left ventricle at the level of the papillary muscles and two-dimensionally guided M-mode recordings through the anterior and posterior walls of the left ventricle were obtained. Left ventricular end-systolic (LVDs) and end-diastolic (LVDd) dimensions as well as thickness of the interventricular septum (IVS) and left ventricular posterior wall (LVPW) in diastole (d) and systole (s) were measured from the M-mode tracings. Left ventricular

shortening fraction (LVFS) was calculated from the M-mode left ventricular dimensions using the following equation: LVFS (%) =  $[(LVDd-LVDs) / LVDd] \times 100$ . Ejection fraction (EF) was also calculated from the M-mode dimensions using the equation: EF (%) =  $[(LVDd)^3 - (LVDs)^3 / LVDd^3] \times 100$ . Functional left ventricular mass was calculated using the equation: LVmass =  $1.055 \times [(IVSd + LVDd + LVDd)] \times (IVDd^3]$ . All the measurements were made from three subsequent cycles and calculated as the mean of these three measurements. Results are expressed as mean  $\pm SD$ .

Function of the mitral, tricuspidal, aortic and pulmonary valves was evaluated by using color flow mapping and pulsed Doppler.

Telemetric analysis. During the telemetric measurements, the mice were housed one per cage in a thermostatically controlled environment at 23±2°C and relative humidity of 50-70%. Mice were allowed free access to chow and drinking water, available ad libitum. The room was artificially illuminated from 7am to 7pm. The heart rate and mean arterial pressure were recorded from the left carotid artery using TA11PA-C20 telemetric implants as previously described, except that xylazine instead of promazine was used for anaesthesia<sup>7</sup>. Mice were allowed a recovery period after surgery and data collection was started on the fifth day when the normal daily circadian rhythm of the mice had returned. The data were sampled continuously day and night for two weeks, every 5 min for 10 s. The presented values, average ± SD, are from a 24-hour period during the fifth day after the start of the measurements. No significant changes were noted in the telemetric variables, 24 h mean daily values of the blood pressure, or heart rate after the fifth day.

Measurements of mitochondrial redox state and tolerance of short-term ischemia in the isolated, perfused hearts. The mice were sacrificed by decapitation after cervical dislocation. The aorta was

immediately cannulated and perfusion commenced in situ with ice-cold perfusion fluid. The heart was dissected out and perfusion continued with Krebs-Henseleit buffer consisting of 118.5 mmol/L NaCl, 4.7 mmol/L KCl, 2.5 mmol/L CaCl<sub>2</sub>, 0.25 mmol/L Ca-EDTA, 1.2 mmol/L MgSO<sub>4</sub>, 1.2 mM KH<sub>2</sub>PO<sub>4</sub>, 25 mmol/L NaHCO<sub>3</sub> and 10 mmol/L glucose (pH 7.4, 37°C) with a pressure of 100 cm H<sub>2</sub>O (9.81 kPa) and the medium gassed with O<sub>2</sub>/CO<sub>2</sub> (19:1).

The heart was enclosed in a thermostatic, light-tight chamber equipped with fiber optics for simultaneous epicardial readout of reflectance spectrum changes at 605 and 630 nm and fluorescence at 520 nm with excitation at 460 nm by means of a three-channel spectrophotometer-fluorometer. The photometric data were collected via a data acquisition card (PCI-6024E, National Instruments) and stored on a PC at two-second intervals. Left ventricular pressure was monitored through the ventricular wall by inserting a saline-filled Teflon cannula connected to a Statham P231D pressure transducer linked to a Statham SP1400 pressure monitor. The pressure wave signal was led to a Lab-PC+ data acquisition card (National Instruments) and heart function parameters (heart rate, peak systolic pressure, diastolic pressure and peak pressure development) were calculated on-line with custom designed software and stored on a PC at 4 s intervals. Coronary flow was measured during the experiments by using a drop counter with an analog output. Oxygen consumption was calculated from the arteriovenous concentration difference multiplied by coronary flow. Venous effluent from the heart was collected in 1 min aliquots and lactate dehydrogenase washout measured as described. The values are presented as mean ± SE.

Angiotensin II-induced pressure overload. AngII was administered to mice via subcutaneous osmotic Alzet minipumps (Scanbur AB) for 1 week (0,1 mg/kg/h). Mice were sacrificed one week later.

Echocardiographic analysis of cardiac dimensions was carried out before the treatment and before sacrifice using a Vevo 779 high-resolution in vivo imaging system (VisualSonics).

Electron microscopy. Tissue samples from the left ventricle were fixed with 2.5% glutaraldehyde, postosmicated and embedded in epon. Semithin sections were stained with toluidine blue, and on the basis of initial analysis under light microscope, regions of interest were selected for thin 100 nm sectioning and analysis using a JEOL 1400 EX Transmission Electron Microscope equipped with Morada CCD Camera (Olympus SIS).

Lipidomic analysis of heart tissue. Hearts were perfused with PBS upon excision, dissected, and snap-frozen. Corresponding pieces (5-9 mg) were mixed with an internal standard mixture containing 1-heptadecanoyl-sn-glycero-3-phosphocholine, N-(heptadecanoyl)-sphing-4-enine, 1,2-diheptadecanoyl-sn-glycero-3-phosphocholine, 1,2-diheptadecanoyl-sn-glycero-3-phosphoethanolamine and 1,2,3-triheptadecanoyl-sn-glycerol at a concentration level of 0.5-1 μg/sample and 200 μl chloroform:methanol (2:1). The tissues were homogenized with grinding balls in a Mixer MILL at 25 Hz for 2 min and 50 μl of 0.9% NaCl was added. The samples were vortexed for 2 min and after 30 min standing, centrifuged at 10 000 rpm for 3 min. The labeled lipid standard mixture was added into the separated lipid extracts (1 μg/sample) before ultra performance liquid chromatography-mass spectrometric analysis.

Lipid extracts were analyzed on a Waters Q-Tof Premier mass spectrometer (Waters, Inc., Milford, MA) combined with an Acquity Ultra Performance LC<sup>TM</sup> (UPLC). The column (at 50°C) was an Acquity UPLC<sup>TM</sup> BEH C18 10 x 50 mm with 1.7 μm particles. The solvent system included A. ultrapure water (1% 1M NH<sub>4</sub>Ac, 0.1% HCOOH) and B. LC/MS grade acetonitrile/isopropanol (5:2, 1%).

1M NH<sub>4</sub>Ac, 0.1% HCOOH). The gradient started from 65% A / 35% B, reached 100% B in 6 min and remained there for the next 7 min. There was a 5 min re-equilibration step before the next run. The flow rate was 0.200 ml/min and the injected amount 1.0  $\mu$ l (Acquity Sample Organizer, Waters, Inc., Milford, MA). Reserpine was used as the lock spray reference compound. The lipid profiling was carried out using ESI+ mode and the data was collected at mass range of m/z 300-1200 with scan duration of 0.2 sec. The data was processed by using MZmine software v. 0.60  $^{10}$  and the lipid identification was based on an internal spectral library  $^{11}$ . Results are presented as mean  $\pm$  SEM.

Statistical analysis of data. Two-group comparison was made with the Student's two-tailed t-test by using the method of summary measures<sup>12</sup> when appropriate.

## References

- 1. Detmar M, Brown LF, Schon MP, Elicker BM, Velasco P, Richard L, Fukumura D, Monsky W, Claffey KP, Jain RK. Increased microvascular density and enhanced leukocyte rolling and adhesion in the skin of VEGF transgenic mice. *J Invest Dermatol*. 1998;111(1):1-6.
- 2. Odorisio T, Schietroma C, Zaccaria ML, Cianfarani F, Tiveron C, Tatangelo L, Failla CM, Zambruno G. Mice overexpressing placenta growth factor exhibit increased vascularization and vessel permeability. *J Cell Sci.* 2002;115(Pt 12):2559-2567.
- 3. Jeltsch M, Kaipainen A, Joukov V, Meng X, Lakso M, Rauvala H, Swartz M, Fukumura D, Jain RK, Alitalo K. Hyperplasia of lymphatic vessels in VEGF-C transgenic mice. *Science*. 1997;276(5317):1423-1425.
- 4. Veikkola T, Jussila L, Makinen T, Karpanen T, Jeltsch M, Petrova TV, Kubo H, Thurston G, McDonald DM, Achen MG, Stacker SA, Alitalo K. Signalling via vascular endothelial growth factor receptor-3 is sufficient for lymphangiogenesis in transgenic mice. EMBO J. 2001;20:1223-1231.
- Vassar R, Rosenberg M, Ross S, Tyner A, Fuchs E. Tissue-specific and differentiation-specific expression of a human K14 keratin gene in transgenic mice. *Proc. Natl. Acad. Sci. USA*. 1989;86:1563-1567.
- 6. Olofsson B, Pajusola K, Kaipainen A, von Euler G, Joukov V, Saksela O, Orpana A, Pettersson RF, Alitalo K, Eriksson U. Vascular endothelial growth factor B, a novel growth factor for endothelial cells. *Proc. Natl Acad. Sci. USA.* 1996;93:2576-2581.
- **7.** Butz GM, Davisson RL. Long-term telemetric measurement of cardiovascular parameters in awake mice: a physiological genomics tool. *Physiol Genomics*. 2001;5(2):89-97.

- 8. Hassinen IE. Reflectance spectrophotometric and surface fluorometric methods for measuring the redox state of nicotinamide nucleotides and flavins in intact tissues. *Methods Enzymol*. 1986;123:311-320.
- 9. Bergmeyer H, Bernt E. Lactat-Dehydrogenase. UV-Test mit Pyruvat und NADH. Methoden der enzymatischen Analyse. Bergmeyer HU (Ed.) Verlag Chemie, Weinberg, Germany. 1970:533-538.
- **10.** Katajamaa M, Oresic M. Processing methods for differential analysis of LC/MS profile data. *BMC Bioinformatics*. 2005;6:179.
- 11. Yetukuri L, Katajamaa M, Medina-Gomez G, Seppanen-Laakso T, Vidal-Puig A, Oresic M. Bioinformatics strategies for lipidomics analysis: characterization of obesity related hepatic steatosis. *BMC Syst Biol.* 2007;1:12.
- **12.** Matthews JN, Altman DG, Campbell MJ, Royston P. Analysis of serial measurements in medical research. *Bmj.* 1990;300(6719):230-235.